Available online at www.sciencedirect.com
ScienceDirect
Virology 358 (2007) 109–118
VIROLOGY
www.elsevier.com/locate/yviro

Modeling-based characterization of the elicitor function of amino acid 461 of *Cucumber mosaic virus* 1a protein in the hypersensitive response

Katalin Salánki [a,1,2], Ákos Gellért [b,*,1], Gábor Náray-Szabó [c], Ervin Balázs [b]

[a] *Agricultural Biotechnology Center, Szent-Györgyi Albert u. 4, H-2100 Gödöllő, Hungary*
[b] *Agricultural Research Institute of the Hungarian Academy of Sciences, Brunszvik út 2, H-2462 Martonvásár, Hungary*
[c] *Protein Modeling Group, Hungarian Academy of Sciences-Eötvös Loránd University, Pázmány Péter stny, 1/A, H-1117 Budapest, Hungary*

Received 19 May 2006; returned to author for revision 20 June 2006; accepted 1 August 2006
Available online 20 September 2006

Abstract

The Ns strain of *Cucumber mosaic virus* (CMV) induces hypersensitive response (HR) on *Nicotiana tabacum* cv. Xanthi-nc and on *Nicotiana glutinosa*. The genetic determinant of the HR induction was localized earlier to amino acid 461 of the 1a protein. The 3D structure of the 1a protein is still unknown and building a homology model is impossible. Nevertheless, on the basis of secondary structure predictions we have created partial protein models for the region surrounding residue 461 which can account structurally for the effect of aa 461 on elicitor function. Seven different amino acid mutations were designed and introduced to the position 461 of the 1a protein in RNA 1. Three of the mutations (proline, glutamic acid, asparagine) inhibited virus replication. Two of the mutants caused systemic symptom development (lysine and arginine). Two mutants (alanine and serine) resulted in localization of the virus, but strong necrosis similar to the original Ns-CMV strain was not observed. Inoculation of purified Ns-CMV virions at extremely high concentration provoked systemic symptoms.

Keywords: Secondary structure prediction; Sequence analysis; Model building; Protein engineering; Electrostatic potential analysis; Plant virology; Cucumber mosaic virus; Cucumoviruses

Introduction

A plant virus infection can result in various host responses. In compatible plant–virus interactions the virus invades the whole plant, resulting in systemic infection and generally provoking systemic symptoms. In incompatible plant–virus combinations the host plant can evade the virus infection at different levels. For example, the virus may not be able to associate with host-specific proteins for replication in the initially infected cell (Hamamoto et al., 1997), or viral cell-to-cell or long distance transport may be non-functional (Ryu et al., 1998; Mise et al., 1993). In the case of a hypersensitive response (HR) the plant avoids systemic infection by localizing the virus or other pathogen to the primary infection site and this defense mechanism is often accompanied by development of necrotic local lesions. In this case, just after virus infection the plant is believed to recognize certain pathogen elicitors (called avirulence [Avr] factors) which activate the defense response. In different virus–host combinations either the RNA-dependent RNA polymerase (Abbink et al., 2001; Erickson et al., 1999), the coat protein (Bendahmane et al., 1995; Taraporewala and Culver, 1996; Gilardi et al., 2004) or the movement protein (Meshi et al., 1989; Weber et al., 1993; Scholthof et al., 1995) has been identified as avirulence determinants, and in one case the viral RNA was shown to be the elicitor of the HR (Szittya and Burgyán, 2001).

Cucumber mosaic virus (CMV), a member of the family Bromoviridae (genus *Cucumovirus*), has an extremely wide host range, including more than 1200 plant species in 500 genera of 100 families. The genome of CMV consists of three positive sense RNA molecules. RNA 1 codes for the 1a protein, which bears putative methyltransferase and helicase domains.

* Corresponding author. Fax: +36 22 569 514.
E-mail addresses: salanki@abc.hu (K. Salánki), gellerta@mail.mgki.hu (Á. Gellért).
[1] These two authors contributed equally to this paper.
[2] Fax: +36 28 526 192.

0042-6822/$ - see front matter © 2006 Elsevier Inc. All rights reserved.
doi:10.1016/j.virol.2006.08.014

RNA 2 bears two overlapping open reading frames that are translated into the 2a protein, which has a polymerase domain, and the 2b protein, which is responsible for suppression of post transcriptional gene silencing and symptom severity. RNA 3 encodes the 3a movement protein and the coat protein (reviewed by Palukaitis and García-Arenal, 2003).

Of these five proteins, three have been identified as Avr proteins on different hosts. The coat protein of the Y strain of CMV was shown to act as the elicitor of the HR on the C24 ecotype of *Arabidopsis thaliana*, and the single dominant locus RCY1 on chromosome 5 of was responsible for this resistance (Takahashi et al., 2001). A requirement for functional salicylic acid (SA)-, jasmonic acid (JA)- and ethylene (ET)-signaling pathways was demonstrated in RCY1-mediated resistance (Takahashi et al., 2002, 2004). The HR on cowpea has been mapped to codons 631 and 641 of the viral polymerase gene, and virus accumulation levels were affected in single infected cells (Kim and Palukaitis, 1997). The Ns isolate of *Cucumber mosaic virus* (CMV) induces necrotic lesions on several *Nicotiana* plants while Rs-CMV causes systemic mosaic symptoms on these plants. The Avr protein was shown to be the 1a protein, and the symptom phenotype was solely determined by amino acid (aa) 461 (Divéki et al., 2004). The 1a protein of Ns-CMV contains a cysteine at position 461 while an arginine is present at this position in Rs-CMV.

Predicted secondary structures of methyltransferase/helicase (1a) proteins of different Sindbis-like (Bromo-, Cucumo-, Tobamoviruses) RNA viruses are very similar (O'Reilly et al., 1998) but no three-dimensional structure of any 1a protein is available. We have nevertheless attempted to find a structural explanation for why the biological properties of the 1a protein are so sensitive to the identity of the aa at position 461. To this end we have developed a partial structural model for the region immediately surrounding residue 461, and have obtained input this model by characterizing the 1a protein elicitor function following designed mutations. Mutants of previously described biologically active cDNA clones of Ns-CMV were used (Divéki et al., 2004) and residue 461 aa of the RNA 1-encoded 1a protein was targeted for mutations. The secondary structure prediction suggested that residue 461 is involved in a basic-neutral amphiphilic α-helix. Based on our mutation experiments and electrostatic considerations we can conclude that conservation of the integrity and amphiphilic character of this helix is essential for virus replication, suggesting that aa 461 of the Ns- and the Rs-CMV 1a protein should play an important role in an active site which is relevant in symptom-forming biochemical processes.

Results

Molecular modeling-based mutation design

Before designing mutations at position 461, we performed secondary structure predictions on the 1a protein with two methods (PHD, PROF). These methods use profile-based neural network prediction from multiple sequence alignments. Both methods predict that residue 461 is the second residue in a 12 residue long α-helix (helix B; Fig. 1B). Just upstream lies another α-helical region (helix A) which is separated from helix B by proline 459, so that the region defined by aa 443–472 (helix AB) may be considered as a bent or interrupted α-helix

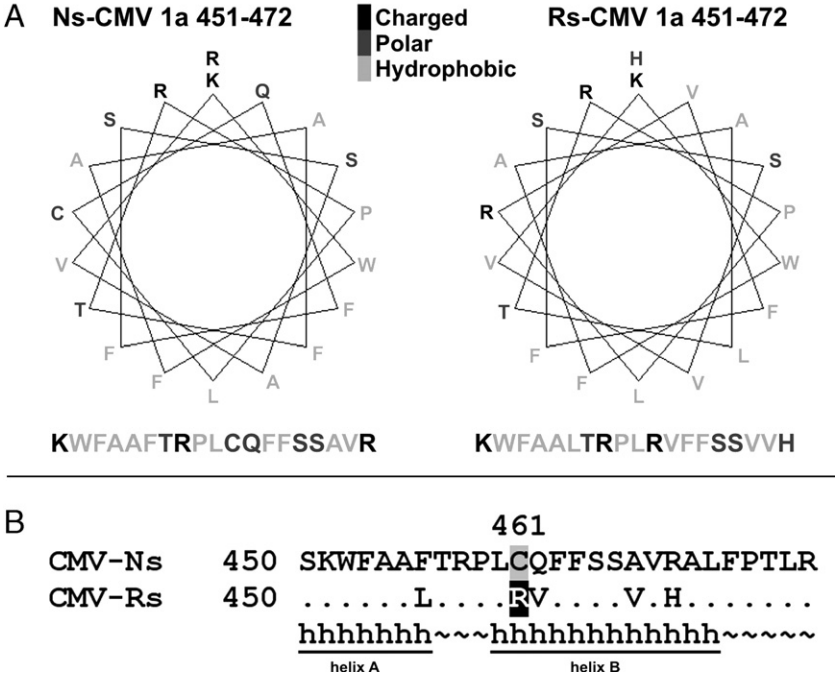

Fig. 1. (A) Helix wheel representation of the Ns- and the Rs-CMV 1a protein sequences between residues 443–472. Color keys are indicated on the figure. (B) Amino acid alignment of the Ns- and Rs-CMV 1a protein sequences between residues 443–472 and the predicted secondary structure of this region. The dots indicate amino acid identity, h represents α-helices, ~ represents loops. Gray background shading indicates C461, and black background shading R461.

(Fig. 1A). Consideration of the distribution of residues on this structure reveals that the hydrophobic residues are essentially located on one face of the helix while the other face contains basic and neutral residues (Fig. 1A). Thus the region containing helices A and B can be considered as an amphiphilic bent α-helix.

Based on this model, residue 461 is at the interface between the hydrophobic and neutral-hydrophilic faces of the extended helix so that it can be substituted by either a positively charged or a neutral residue without changing the amphiphilic nature of the structure. In view of this hypothesis we designed seven point mutations to investigate the role of residue 461. All mutations were carried out on the 1a protein of the Ns-CMV. The first mutation was C461A where we replaced C461 by a neutral alanine. The second mutation was C461S, to test an earlier hypothesis that C461 can participate in an intra- or intermolecular disulphide bond and that this is needed for necrosis induction (Divéki et al., 2004). The third mutation was C461R, the substitution observed in the non-necrogenic strain Rs-CMV. The forth mutation was C461K, to determine if a positively charged residue other than R at this position produces similar symptoms to the Rs-CMV. The fifth mutant was C461P. Here the proline residue is expected to break the abovementioned helix. The sixth mutation was C461N, to determine the effect of a hydrophilic and polar aa at position 461. Finally, the seventh mutation was C461E. The glutamic acid with its negative charge should abolish the helix amphiphilicity.

Infectivity of the mutant clones on N. clevelandii protoplasts and plants

The replication characteristics of the RNA 1 mutants were analyzed in *N. clevelandii* protoplasts in the presence of RNA 2 and 3 of Ns-CMV (Fig. 2). Northern analysis of the infected protoplasts revealed the replication incompetence of the nC461E, nC461P and nC461N mutants 24 h after infection. All the other mutants were able to replicate although the replication of the nC461K mutant was less efficient than the others. We conclude that the mutations which are predicted to disorganize the putative α-helix (443–472) (C461P) or to destroy its amphiphilic character (nC461E) inhibit the function of 1a in replication.

Infection of N. clevelandii plants

Since Ns-CMV and Rs-CMV both infect *N. clevelandii* systemically, we chose this host for the initial infection experiments. *In vitro* transcripts of all the mutated clones were infected in the presence of the RNA 2 and 3 transcripts of Ns-CMV. Symptom appearance was monitored visually and RT/PCR analysis was carried out to confirm the infection. The mutants nC461E, nC461P and nC461N did not provoke an infection, as was expected from the results of the protoplast experiments. In the case of wild-type Ns-CMV and the mutants nC461R, nC461S, nC461A, systemic symptoms appeared 5–6 days after infection, while in the case of nC461K the symptoms delayed, appearing only 10–12 days after infection. The RT/PCR analysis confirmed the visual observations. We purified virions from the infected plants 10–14 days after inoculation. The efficiency of virus purification was similar for the different mutants. We extracted viral RNA from the purified viruses, and the nucleotide sequence of the nt 1324–2400 fragment of RNA 1 was determined directly on the RT/PCR product. All the introduced mutations were retained in the purified viruses, and no other mutations were observed.

The pathological characteristics of the RNA 1 mutants

Purified virions at a concentration of 50 μg/ml were used as inoculum for further infection experiments. The Ns-CMV isolate induced necrotic lesions on the inoculated leaves of *Nicotiana tabacum* cv. Xanthi-nc and on *N. glutinosa*, while the Rs-CMV isolate and the nC461R mutant caused systemic

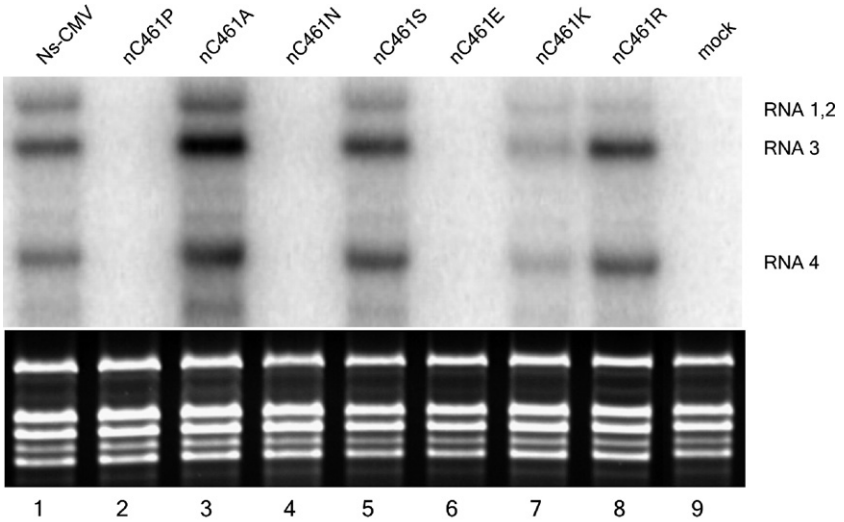

Fig. 2. Progeny analysis of *N. clevelandii* protoplasts inoculated with the *in vitro* transcripts of different chimeras in the presence of pN1 and pN2 transcripts. The radiolabeled probe was specific for the 3′-end of CMV RNA 3. Ribosomal RNAs stained with ethidium bromide are shown to illustrate equal loading of samples.

Table 1
Summary results of the experiments on plant species

1a Protein variants	Plant species inoculated[a]					
	Nicotiana clevelandii		*Nicotiana glutinosa*		*Nicotiana tabacum* cv. Xanthi	
	Inoculated	Systemic	Inoculated	Systemic	Inoculated	Systemic
Ns-CMV	L.	M.	Low conc.: L.	–	Low conc.: L.	–
			High conc.: L.	M.	High conc.: L.	M.
Rs-CMV	M.	M.	Low conc.: M.	M. 4 d.p.i.	Low conc.: M.	M. 4. d.p.i.
			High conc.: M.	M. 4 d.p.i.	High conc.: M.	M. 4. d.p.i.
nC461A	L.	M.	Low conc.: L.	–	Low conc.: L.	–
			High conc.: L.	–	High conc.: L.	–
nC461S	L.	M.	Low conc.: L.	–	Low conc.: L.	–
			High conc.: L.	Chlorosis	High conc.: L.	Chlorosis
nC461K	M.	M. 8 d.p.i.	Low conc.: M.	M. 8 d.p.i.	Low conc.: M.	M. 8 d.p.i.
			High conc.: M.	M. 8 d.p.i.	High conc.: M.	M. 8 d.p.i.
nC461R	M.	M. 4 d.p.i.	Low conc.: M.	M. 4 d.p.i.	Low conc.: M.	M. 4 d.p.i.
			High conc.: M.	M. 4 d.p.i.	High conc.: M.	M. 4 d.p.i.
nC461P	–	–	–	–	–	–
nC461N	–	–	–	–	–	–
nC461E	–	–	–	–	–	–

[a] L.=Lesion, M.=Mosaic, conc.=concentration, d.p.i.: days post-inoculation.

mosaic symptoms on these hosts and did not induce necrotic lesions on the inoculated leaves (Divéki et al., 2004). Local lesions developed on the inoculated leaves infected with the mutant clones nC461S and nC461A, but systemic infection was not observed (Table 1). Northern analysis of the upper non-inoculated leaves supported the visual observation (Fig. 3). The phenotypes of the local lesions were distinct in the case of the different mutants (Figs. 4, 5) even though they developed at similar rates. On *N. tabacum* cv. Xanthi-nc, the lesions caused by wild Ns-CMV necrotized completely and were surrounded by one or more "etched" lines (Fig. 4A). In the case of nC461A, the middle of the lesions was not necrotized, and the etched line pattern was highly developed (Fig. 4C). The etched line pattern in the case of the nC461S was less well defined and necrosis was not induced (Fig. 4E). On *N. glutinosa* the lesions were necrotic spots with Ns-CMV and nC461A (Figs. 5A, C), although the outline of the lesion was less well defined in the latter case. The lesions in the case of the mutant nC461S were not necrotized (Fig. 5E).

The mutant nC461K caused systemic mosaic symptom similar to nC461R, but the systemic symptoms developed 3–4 days later. Systemic symptom development of the inoculated *N. tabacum* cv. Xanthi plants was monitored by Northern analysis (Fig. 3). While we could detect both Rs-CMV and nC461R progeny RNA in the upper non-infected leaves of the test plant four days after inoculation, the nC461K progeny RNA appeared only 8 days after inoculation.

To analyze the impact of extremely high virus concentration, we inoculated the test plants with a virus concentration of 5 mg/ml. The results of all the infections were similar on *N. tabacum* cv. Xanthi and *N. glutinosa*. In the case of the systemically infectious mutants the infection phenotype did not

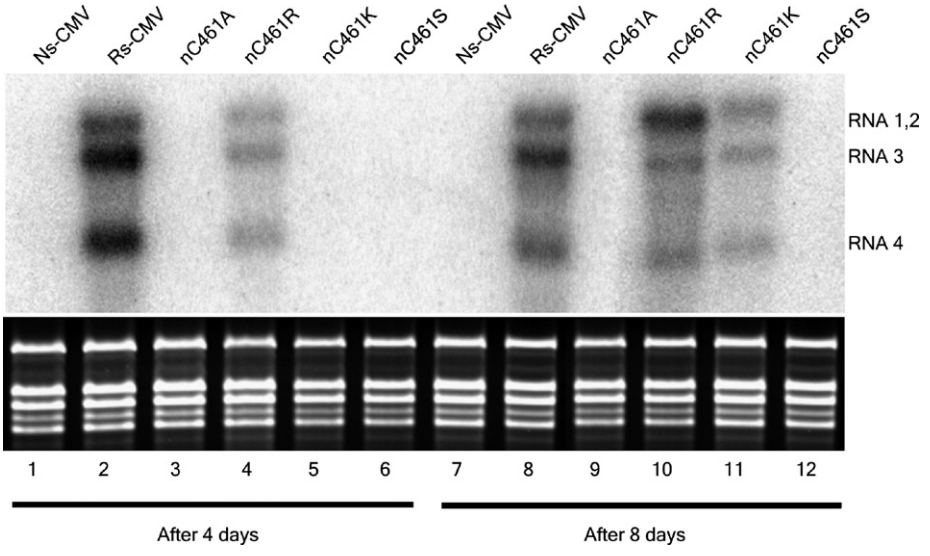

Fig. 3. Northern blot hybridization analysis of systemically infected leaves of *Nicotiana tabacum* cv. Xanthi-nc plants. The radiolabeled probe was specific for the 3′-end of CMV RNA 3. Ethidium–bromide-stained rRNA from the same volume of each sample is shown below each lane.

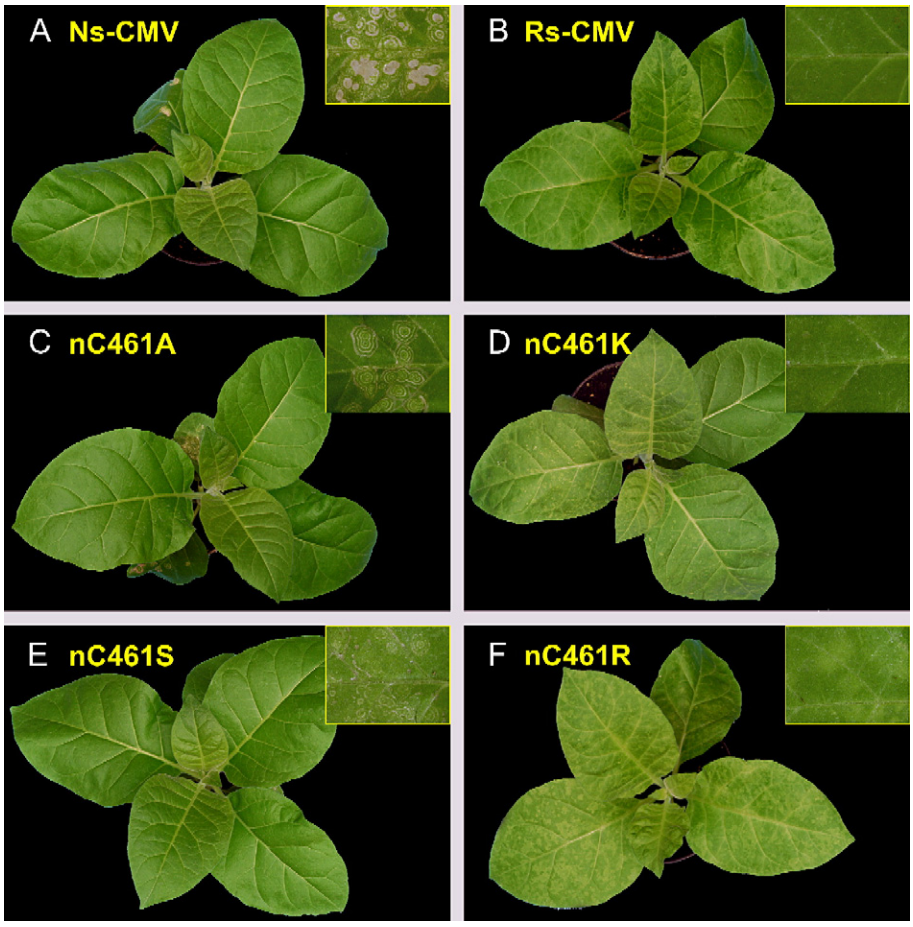

Fig. 4. Local and systemic symptoms induced by the wild type (A: Ns-CMV, B: Rs-CMV) and the different mutants (C: nC461A, D: nC461K, E: nC461S and F: nC461R) on *Nicotiana tabacum* cv. Xanthi-nc plants, at 2 weeks p.i. The local symptoms are shown in the upper corner of each photo. The plants were inoculated with purified virions at a concentration of 50 μg/ml.

change. For the mutants causing local lesions, quick collapse of the infected leaves occurred, and with the mutant nC461A systemic symptom development was never observed. In the case of Ns-CMV, systemic mosaic symptom was induced (data not shown), and nucleotide sequence analysis after RT/PCR amplification proved that these symptoms were not associated with nucleotide changes in the region of interest. We also inoculated test plants with diluted plant sap from the systemically Ns-CMV infected leaves, and the original local lesion symptoms developed without systemic symptoms. Infection with the nC461S mutant sometimes resulted unusual systemic symptoms on a few upper leaves. Yellow patches appeared around some veins, but the virus was restricted to a small part of the leaf (Fig. 6). The presence of the mutant virus sequence was confirmed by nucleotide sequence determination of the RT/PCR product. In the green area of the leaves virus was not detectable by either Northern analysis or RT/PCR reaction.

Effects of the mutations on 1a protein structure and function

As noted above, computer-based secondary structure predictions indicate that there are two amphiphilic α-helix parts in the Ns- and Rs-CMV 1a protein structure between residues 443 to 472, with P459 breaking in the continuous helix thread (Fig. 7). There are numerous amino acids with hydrophobic side chains on one side of this putative bent helix and on the other side there are amino acids with basic side chains, so that the region in question is predicted to be a neutral-basic bent amphiphilic α-helix. Position 461 localizes at the boundary of the amphiphilicity suggesting that this residue could play an important role in the function of the 1a protein.

In the case of the nC461P mutant, we performed a short (200 ps) molecular dynamic simulation and the structure of this bent amphiphilic α-helix was predicted to be changed significantly, as we expected. In the case of nC461E mutant the amphiphilic character of the bent helix is diminished due to the negative charge of the glutamic acid (Fig. 7H). The protoplast infection experiments show that these mutations disabled replication. The nC461A and nC461S mutants cause the same symptoms as the wild-type Ns-CMV isolate and are not predicted to change the integrity and amphiphilicity of the helix. Mutations nC461K and nC461R caused similar mosaic symptoms as the Rs-CMV. These mutations introduced a different aa on the boundary between the hydrophilic and hydrophobic sides of the helix, but they do not change overall helix integrity and amphiphilic character. The C461K mutant provokes symptoms similar to the Rs isolate, which has the C461R substitution. Finally in the case of mutation nC461N,

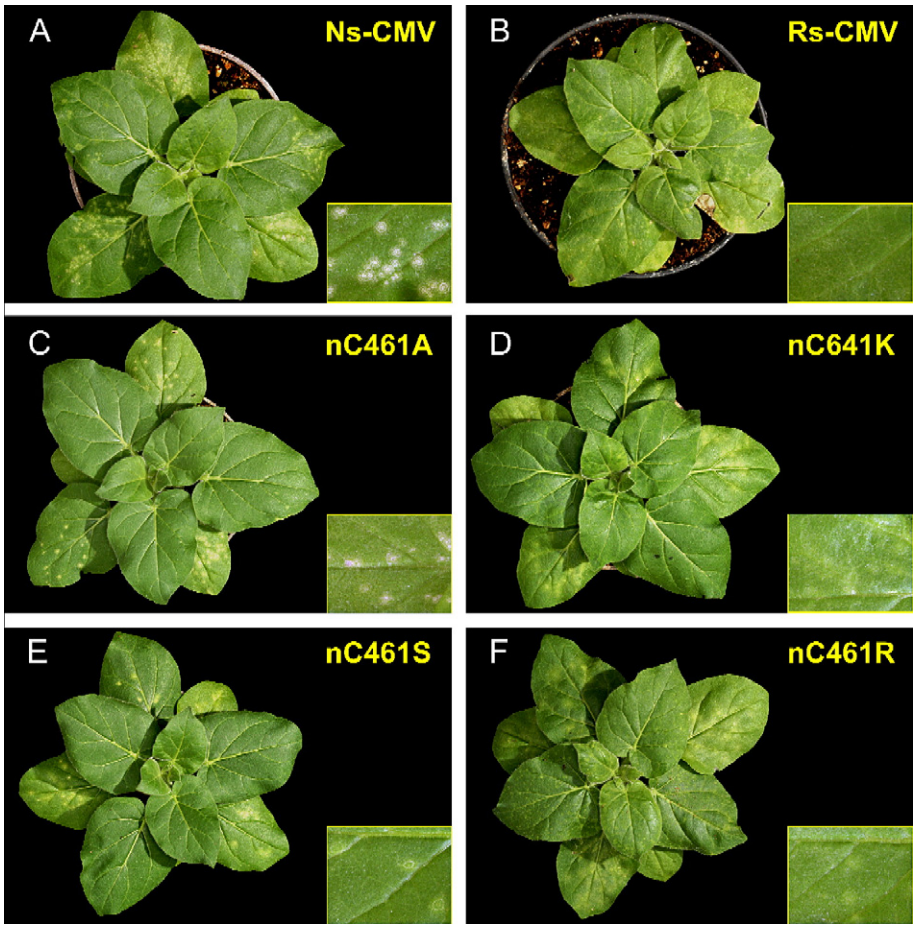

Fig. 5. Systemic symptoms provoked by the wild type (A: Ns-CMV, B: Rs-CMV) and the different mutants (C: nC461A, D: nC461K, E: nC461S and F: nC461R) on *Nicotiana glutinosa* plants, at 2 weeks p.i. The local symptoms are shown in the lower corner of each photo. The plants were inoculated with purified virions at a concentration of 50 μg/ml.

although the structure and electrostatic properties of the examined region did not change, this mutant nevertheless did not replicate.

Discussion

The use of structural biology and protein modeling in plant virus research has the potential to provide a better understanding of the structural basis of biological phenomena. Structure–function relationships can be analyzed with high confidence in the case of proteins which structures are known. Thus for cucumoviruses the three-dimensional structures of the coat proteins of the Fny-CMV and the Blencowe strain of TAV (*Tomato aspermy virus*) have been determined by X-ray crystallography (Smith et al., 2000; Lucas et al., 2002). Using homology modeling, structures were predicted for related CMV and TAV coat proteins (Salánki et al., 2004; Gellért et al., 2006; Pacios and García-Arenal, 2006; Llamas et al., 2006). Building

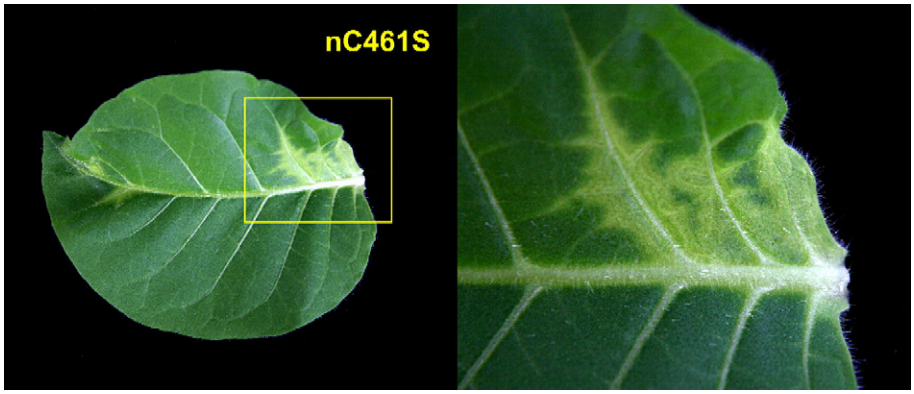

Fig. 6. Systemic symptoms provoked by the nC461S mutant at 18 days p.i. The plant was inoculated with purified virions at a concentration of 50 mg/ml.

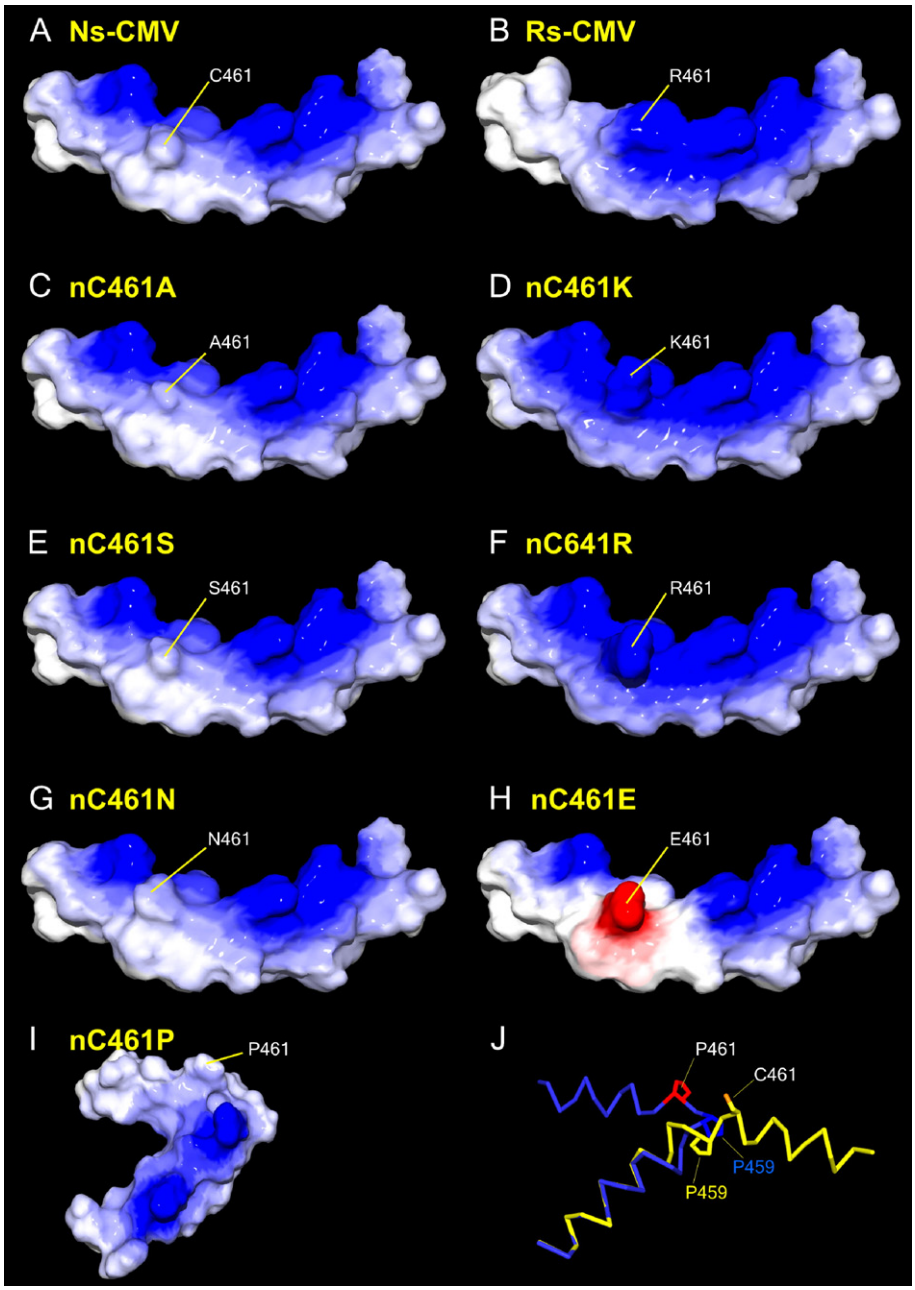

Fig. 7. Mutation effects on 1a protein structure and function. All models represent the predicted amphiphilic α-helical substructure of the 1a protein from residue 443 to 472. (A) Wild-type Ns-CMV 1a; (B) wild-type Rs-CMV 1a. (C) C461A, (D) C461K, (E) C461S, (F) C461R, (G) C461N, (H) C461E and (I) C461P mutations of the Ns-CMV 1a protein. (J) A possible deformed conformation of this substructure in the case of the C461P mutant. (A–I) Red, regions with potential less than −1.8 kT; white, 0.0; blue, greater than +1.8 kT.

a homology model for the 1a protein is impossible because there are no prototype protein structures in the PDB database (http://www.rcsb.org/pdb) where the sequence similarity is larger than 20–30%. The use of other protein structure computing methods such as "ab initio structure modeling" or "fold recognition with threading" is also rather limited due to the large size of the 1a protein (111 kDa, 993 aa). In the case of 1a protein, however, were able to use secondary structure predictions to create a partial protein models (α-helices) for the region immediately surrounding residue 461, and deigned targeted mutations to test the model in this region.

The mutations which were predicted to strongly change the protein structure (C461P) or disrupt the surface electrostatic potential pattern (C461E) disabled replication of CMV. Position 461 is localized on the boundary between the hydrophilic and hydrophobic faces of the helix located between aa 443 and 472 of the 1a protein. Proline is known to be a helix breaking aa, so it is expected that the integrity of the helix would be damaged and in consequence the general protein structure would be altered. In C462E, a negative charge is introduced. Even though the computer predictions indicate that the helix integrity and the hydrophobic face remain unaffected, the presence of this changed

residue also inhibits replication. The C461N mutation was also replication-incompetent, an unexpected result since this mutation was not predicted to provoke major secondary structure changes.

Conformational and functional information on the CMV 1a protein is mainly based on data gained by the detailed analysis of the closely related *Brome mosaic virus* (BMV). Despite low amino acid similarity (55%), CMV and BMV 1a proteins probably share similar structural features. Both structures, however, are still unknown. Homologous regions containing the position 461 of CMV and BMV locate in the middle of an α-helix in the capping domain of the protein (O'Reilly et al., 1998), in the sequence determinant responsible for membrane association (den Boon et al., 2001). A perfect correlation was observed between the maintenance of the predicted secondary structure and the ability to replicate in protoplasts in the case of BMV, that is, all of the non-replicating mutants were predicted to have an adverse effect on the structure of their region (O'Reilly et al., 1998). In our experiments the replication-incompetent mutant C461N retained the original predicted structure and amphiphilicity, so presumably the membrane association and the overall structure of the protein is maintained. These results suggest that this region of the 1a protein is exposed on the surface of the protein and has a direct and crucial role in virus replication.

All the other mutants (C461A, C461S, C461K, C461R) were replication competent in *N. clevelandii* protoplasts, but generally two different biochemical pathways were induced. Systemic mosaic symptoms were observed for mutants in which the introduced amino acid has a positively charged side chain (C461K, C461R), even if the replication of the C461K was not as efficient as in the case of the other replication-competent strains. The C461K mutant induced systemic mosaic symptoms 3–4 days later than the C461R mutant, probably due to its slower replication rate. It may be noteworthy that the side chain of arginine has a higher pK_a value than lysine.

The Ns-CMV, the C461A and the C461S mutants induced hypersensitive response on *N. tabacum* cv. Xanthi and on *N. glutinosa* plants. These results prove that disulphide bond formation is not required at position 461 for necrosis induction.

Two different molecular models for the HR have been proposed. In the ligand-receptor model a direct interaction between the Avr and the R protein is required for gene-for-gene resistance (Gabriel and Rolfe, 1990; Keen, 1990). Such an interaction has been elucidated for a few Avr proteins and the corresponding R gene products in the case of different bacteria and fungi (Bonas and Lahaye, 2002; reviewed by Martin et al., 2003). The other model is the so-called guard hypothesis (Nimchuk et al., 2003; Van der Biezen and Jones, 1998), which postulates an indirect interaction between the Avr and the R proteins with host factors (Dangl and Jones, 2001; Schulze-Lefert, 2004). The HR has two key characteristics, cell death within the initially infected tissue and restriction of the pathogen to this area. Recently it was shown in the case of *Cauliflower mosaic virus*-induced HR on *Nicotiana* spp. that the resistance pathway and the cell death pathway can be uncoupled (Cawly et al., 2005) and can be induced selectively (Cole et al., 2001). Kim and Palukaitis (1997) also described the presence of an inhibitory response distinct from the HR in cowpea infected by CMV. Our work supports these observations since striking differences were observed in necrosis induction on the inoculated leaves (C461A, C461S, Ns-CMV) while the resistance phenotype did not change. The C461A and C461S mutations can selectively induce the resistance pathway while the cell death pathway is not triggered. A satisfactory molecular explanation for this phenomenon will require identification of the interacting R protein and the induced pathways, since the key factor probably involves improper protein–protein interactions or protein structural changes after formation of protein–protein complex.

Defense response activation has been reported to depend on temperature (CMV) (Erickson et al., 1999; Taraporewala and Culver, 1996) and on the stage of plant development (*Tobacco mosaic virus*, TMV) (Zheng et al., 2004). Our experiments illustrate the importance of the concentration of virus used as inoculum in activating the defense response. Infecting plants with extremely high virus concentration can result in systemic infection instead of the HR. These results suggest a competition between the HR and the virus infection pathways such that, if the activation of the plant defense system is delayed, the virus is able to systemically infect the host plant (Ns-CMV) and even to completely repress activation of the HR pathway. In other cases the virus can initially escape the defense response, but the defense response later localizes it in a section of the leaf without a necrotic response (C461S). If, on the other hand, the resistance response is strongly activated, the virus was restricted to the site of infection in all the experiments (C461A).

Our results thus demonstrate competition between the pathogen and the plant defense system, and the existence of different pathways during HR since the strongest necrosis and the strongest resistance responses are induced by different mutants. The described host-pathogen system thus provides a good model to identify biochemical pathways differentially responsible for necrosis and virus localization. Our findings also illustrate that molecular modeling and design can provide invaluable input for designing and interpreting plant virology experiments.

Methods and materials

Bioinformatics, model building and electrostatic analysis

The sequences appear in the EMBL/GenBank/DDBF databases under accession numbers CAE45702 and CAD54664 for the Ns-CMV 1a and the Rs-CMV 1a proteins, respectively. Secondary structure predictions were performed for the Ns and Rs 1a protein sequences using the PHD and the PROF (Profile network prediction HeiDelberg) methods (Rost and Sander, 1993, 1994; Rost, 1996). Nine models were built by the SYBYL program corresponding to the secondary structure predictions. All models contain 30 residues from residue 443 to 472, and an acetyl group at the N-terminal, and N-methyl group at the C-terminal for the correct electrostatic calculations. The models were refined with energy minimization using a molecular mechanics force field (Kollman-All-Atom with Kollman charges (Weiner et al., 1984)) incorporated in the SYBYL 6.5 software package. At the beginning of the energy minimization process the steepest descent technique was used to

eliminate steric conflicts between the side-chain atoms until the root mean square (rms) force was reduced to 50 kcal/mol/Å. Once at this threshold, the program automatically continued the energy minimization performing the Powell conjugate gradient optimization until the maximum force became less than 0.05 kcal/mol/Å. We applied a distance dependent dielectric constant ($\varepsilon = 4R$) during the energy minimization. Electrostatic potential maps were calculated by the linearized Poisson–Boltzmann method (Gilson et al., 1987) using dielectric constant values of 80 and 4.0 for the water solvent and protein core, respectively. The ionic strength was fixed at 0.1 mol/l. All Lys (+1), Arg (+1), Glu (−1), Asp (−1) side chains were considered as ionized (actual charges in parentheses). Atomic charges were calculated by the GRASP program (Nicholls et al., 1991). Molecular graphics and the electrostatic potential representations were created by the Swiss PDB Viewer 3.7 (Guex and Peitsch, 1997) using GRASP surface files with electrostatic property. Evaluation of the refined models was carried out with Swiss PDB Viewer 3.7. Model representations were rendered by the POV-Ray 3.5 program (PovRay, 2002).

Viruses, infectious clones, plants and plant maintenance

Rs-CMV, Ns-CMV and the infectious transcripts (pN1, pN2, pN3, pR1, pR2, pR3) derived from these strains were described earlier (Divéki et al., 2004). The test plants were kept in environmentally controlled growth chambers with a cycle of 14 h of light (22 °C) and 10 h of dark (18 °C). *N. glutinosa*, and *N. tabacum* cv. Xanthi-nc was mechanically inoculated at the four-leaf stage, while *Nicotiana clevelandii* was inoculated at the 3 week stage with *in vitro* transcripts or purified virions. Virions at a concentration of 50 μg/ml or 5 mg/ml were used as inoculum. Viruses were propagated on *Nicotiana benthamiana* and purified (Lot et al., 1972) prior to inoculation. In each case, the data represent the results of at least three independent experiments.

Construction of mutants RNA 1

The mutant pC461R was constructed earlier (Divéki et al., 2004). All the other mutant RNA 1 clones were generated by PCR-based site-directed mutagenesis of pN1. Oligonucleotide primers intended to insert point mutations were designed with the SilMut software package (available online from IUBioSoftware Archive). All oligonucleotides contained a *Stu*I restriction endonuclease site as silent mutation. The oligonucleotide 5′-CAGAAGGCCTAGTAAATGCTGCAAACCACTTG-3′ was the reverse primer in all case, while the forward oligonucleotide primers were as follows: for C→K mutation 5′-ACTAGGCCTCTG**AAG**CAGTTTTTCTCTAGTGCTGTTCG-3′, for C→S mutation 5′-ACTAGGCCTCTG**T**C**T**CAGTTTTTCTCTAGTGCTGTTCG-3′, for C→E mutation 5′-ACTAGGCCTCTG-**GAG**CAGTTTTTCTCTAGTGCTGTTCG-3′, for C→N mutation 5′-ACTAGGCCTCTG**AA**TCAGTTTTTCTCTAGTGCTGTTCG-3′, for C→A mutation 5′-ACTAGGCCTCTG-**GC**TCAGTTTTTCTCTAGTGCTGTTCG-3′, for C→P mutation 5′-ACTAGGCCTCTG**CC**TCAGTTTTTCTCTAGTGCTGTTCG-3′ (the *StuI* endonuclease recognition sites are underlined and the mutagenized nucleotides are capitalized). Template was amplified with *Pfu* polymerase to minimize the chance of non-intentionally introduced mutations. PCR products were circularized after cutting with *StuI* endonuclease, and the nucleotide sequences of the mutated clones were confirmed by automated dideoxy sequencing. The names of the mutated clones indicate the mutations: pC461K, pC461S, pC461E, pC461N, pC461A, pC461P.

Protoplast and plant infection with in vitro transcripts

For plant and protoplast inoculation 2 μg transcript of each of the pN1, pR1 or the mutated N1 clones and pN2 and pN3 were used. Protoplasts were isolated from fully expanded *N. clevelandii* leaves and purified in K3 medium containing 0.4 M sucrose (Nagy and Maliga, 1976). Protoplast transfection with RNA transcripts was carried out as described by Kroner and Ahlquist (1992).

Analysis of plants and protoplasts

Total RNAs were extracted from the protoplasts 24 h after infection or from 200 mg fresh leaf tissue 6 days (inoculated leaves) and 14–21 days (systemic leaves) after inoculation (White and Kaper, 1989). Approximately 100 ng RNA was denatured with formaldehyde and formamide, separated in formaldehyde-containing agarose gels and blotted onto nylon membranes (Sambrook et al., 1989). Northern blot hybridization analysis was performed with random-primed, ^{32}P-labeled DNA fragments specific for the 3′ terminal 223nt of the pN1.

RNA was extracted from virions with phenol and SDS. First strand cDNA was synthesized with CMV 3′-end-specific primer and *Avian myeloblastosis virus* reverse transcriptase. PCR amplification was carried out with the 3′-end-specific primer, and with the 5′-GGCGAACGGATAGACATCAATG-3′ primer-specific for nucleotides 1324–1345 of pN1using *Pfu* DNA polymerase. The nucleotide sequence of the PCR product was determined by automated dideoxy sequencing.

Acknowledgments

We thank Júlia Novák Nádudvari for the excellent technical assistance. K. Salánki was supported by the Bolyai János fellowship of the Hungarian Academy of Sciences. The authors are grateful to Dr. K. E. Richards for critical reading of the manuscript. This work was funded by the OTKA-TS44778 Science School grant and by the OTKA-T048683 grant.

References

Abbink, T.E., de Vogel, J., Bol, J.F., Linthorst, H.J., 2001. Induction of a hypersensitive response by chimeric helicase sequences of tobamoviruses U1 and Ob in N-carrying tobacco. Mol. Plant-Microb. Interact. 14, 1086–1095.

Bendahmane, A., Kohn, B.A., Dedi, C., Baulcombe, D.C., 1995. The coat protein of potato virus X is a strain-specific elicitor of Rx1-mediated virus resistance in potato. Plant J. 8, 933–941.

Bonas, U., Lahaye, T., 2002. Plant disease resistance triggered by pathogen-derived molecules: refined models of specific recognition. Curr. Opin. Microbiol. 5, 44–50.

Cawly, J., Cole, A.B., Király, L., Qiu, W., Schoelz, J.E., 2005. The plant gene CCD1 selectively blocks cell death during the hypersensitive response to Cauliflower mosaic virus infection. Mol. Plant-Microb. Interact. 18, 212–219.

Cole, A.B., Király, L., Ross, K., Schoelz, J.E., 2001. Uncoupling resistance from cell death in the hypersensitive response of *Nicotiana* species to cauliflower mosaic virus infection. Mol. Plant-Microb. Interact. 14, 31–41.

Dangl, J.L., Jones, J.D., 2001. Plant pathogens and integrated defense responses to infection. Nature 411, 826–833.

den Boon, J.A., Chen, J., Ahlquist, P., 2001. Identification of sequences in Brome mosaic virus replicase protein 1a that mediate association with endoplasmic reticulum membranes. J. Virol. 75, 12370–12381.

Divéki, Z., Salánki, K., Balázs, E., 2004. The necrotic pathotype of the cucumber mosaic virus (CMV) ns strain is solely determined by amino acid 461 of the 1a protein. Mol. Plant-Microb. Interact. 17, 837–845.

Erickson, F.L., Holzberg, S., Calderon-Urrea, A., Handley, V., Axtell, M., Corr, C., Baker, B., 1999. The helicase domain of the TMV replicase proteins induces the N-mediated defense response in tobacco. Plant J. 18, 67–75.

Gabriel, D.W., Rolfe, B.G., 1990. Working models of specific recognition in plant-microbe interactions. Annu. Rev. Phytopathol. 28, 365–391.

Gellért, Á., Salánki, K., Náray-Szabó, G., Balázs, E., 2006. Homology modelling and protein structure based functional analysis of five cucumovirus coat proteins. J. Mol. Graph. Model. 24, 319–327.

Gilardi, P., Garcia-Luque, I., Serra, M.T., 2004. The coat protein of tobamovirus acts as elicitor of both L2 and L4 gene-mediated resistance in *Capsicum*. J. Gen. Virol. 85, 2077–2085.

Gilson, M.K., Sharp, K.A., Honig, B., 1987. Calculating electrostatic interactions in biomolecules: method and error assessment. J. Comp. Chem. 9, 327–335.

Guex, N., Peitsch, M.C., 1997. SWISS-MODEL and the Swiss-PdbViewer: an environment for comparative protein modeling. Electrophoresis 18, 2714–2723.

Hamamoto, H., Watanabe, Y., Kamada, H., Okada, Y., 1997. A single amino acid substitution in the virus-encoded replicase of tomato mosaic tobamovirus alters host specificity. Mol. Plant-Microb. Interact. 10, 1015–1018.

Keen, N.T., 1990. Gene-for-gene complementarity in plant–pathogen interactions. Annu. Rev. Genet. 24, 447–463.

Kim, C.H., Palukaitis, P., 1997. The plant defense response to cucumber mosaic virus in cowpea is elicited by the viral polymerase gene and affects virus accumulation in single cells. EMBO J. 16, 4060–4068.

Kroner, P., Ahlquist, P., 1992. RNA-based viruses. Molecular Plant Pathology. A Practical Approach, vol. I. IRL Press, Oxford, pp. 23–34.

Llamas, S., Moreno, I.M., García-Arenal, F., 2006. Analysis of the viability of coat-protein hybrids between *Cucumber mosaic virus* and *Tomato aspermy virus*. J. Gen. Virol. 87, 2085–2088.

Lot, H., Marrou, J., Quiot, J.B., Esvan, C., 1972. Contribution á l'étude du virus de la mosaique du concombre (CMV): I. Méthode de purification rapide du virus. Ann. Phytopathol. 4, 25–38.

Lucas, R.W., Larson, S.B., Canady, M.A., McPherson, A., 2002. The structure of *Tomato aspermy virus* by X-ray crystallography. J. Struct. Biol. 139, 90–102.

Martin, G.B., Bogdanove, A.J., Sessa, G., 2003. Understanding the functions of plant disease resistance proteins. Annu. Rev. Plant Biol. 54, 23–61.

Meshi, T., Motoyoshi, F., Maeda, T., Yoshiwoka, S., Watanabe, H., Okada, Y., 1989. Mutations in the tobacco mosaic virus 30-kD protein gene overcome Tm-2 resistance in tomato. Plant Cell 1, 515–522.

Mise, K., Allison, R.F., Janda, M., Ahlquist, P., 1993. Bromovirus movement protein genes play a crucial role in host specificity. J. Virol. 67, 2815–2823.

Nagy, J.I., Maliga, P., 1976. Callus induction and plant regeneration from mesophyll protoplasts of *Nicotiana sylvestris*. Z. Pflanzenphysiol. 78, 453–455.

Nicholls, A., Sharp, K., Honig, B., 1991. Protein folding and association—insights from the interfacial and thermodynamic properties of hydrocarbons. Prot. Struct. Funct. Genet. 11, 281–296.

Nimchuk, Z., Eulgem, T., Holt, B.F., Dangl, J.L., 2003. Recognition and response in the plant immune system. Annu. Rev. Genet. 37, 579–609.

O'Reilly, E.K., Wang, Z., French, R., Kao, C.C., 1998. Interactions between the structural domains of the RNA replication proteins of plant-infecting RNA viruses. J. Virol. 72, 7160–7169.

Pacios, L.F., García-Arenal, F. 2006. Comparison of properties of particles of *Cucumber mosaic virus* and *Tomato aspermy virus* based on the analysis of molecular surfaces of capsids. 87, 2073–2083.

Palukaitis, P., García-Arenal, F., 2003. Cucumoviruses. Adv. Virus Res. 62, 241–323.

PovRay, version 3.5, 2002, POV-Team, Williamstown, Victoria, Australia,

Rost, B., 1996. PHD: predicting one-dimensional protein structure by profile-based neural networks. Methods Enzymol. 266, 525–539.

Rost, B., Sander, C., 1993. Prediction of protein structure at better than 70% accuracy. J. Mol. Biol. 232, 584–599.

Rost, B., Sander, C., 1994. Combining evolutionary information and neural networks to predict protein secondary structure. Proteins 19, 55–72.

Ryu, K.H., Kim, C.H., Palukaitis, P., 1998. The coat protein of cucumber mosaic virus is a host range determinant for infection of maize. Mol. Plant-Microb. Interact. 11, 351–357.

Salánki, K., Gellért, Á., Huppert, E., Náray-Szabó, G., Balázs, E., 2004. Compatibility of the movement protein and the coat protein of cucumoviruses is required for cell-to-cell movement. J. Gen. Virol. 85, 1039–1048.

Sambrook, J., Fritsch, E.F., Maniatis, T., 1989. Molecular Cloning: A Laboratory Manual, 2nd ed. Cold Spring Harbor Laboratory, Cold Spring Harbor, NY, U.S.A.

Scholthof, H.B., Scholthof, K.B., Kikkert, M., Jackson, A.O., 1995. Tomato bushy stunt virus spread is regulated by two nested genes that function in cell-to-cell movement and host-dependent systemic invasion. Virology 213, 425–438.

Schulze-Lefert, P., 2004. Plant immunity: the origami of receptor activation. Curr. Biol. 14, 22–24.

Smith, T.J., Chase, E., Schmidt, T., Perry, K.L., 2000. The structure of cucumber mosaic virus and comparison to cowpea chlorotic mottle virus. J. Virol. 74, 7578–7586.

Szittya, G., Burgyán, J., 2001. Cymbidium ringspot tombusvirus coat protein coding sequence acts as an avirulent RNA. J. Virol. 75, 2411–2420.

Takahashi, H., Suzuki, M., Natsuaki, K., Shigyo, T., Hino, K., Teraoka, T., Hosokawa, D., Ehara, Y., 2001. Mapping the virus and host genes involved in the resistance response in cucumber mosaic virus-infected *Arabidopsis thaliana*. Plant Cell Physiol. 42, 340–347.

Takahashi, H., Miller, J., Nozaki, Y., Sukamto, Takeda, M., Shah, J., Hase, S., Ikegami, M., Ehara, Y., Dinesh-Kumar, S.P., 2002. RCY1, an *Arabidopsis thaliana* RPP8/HRT family resistance gene, conferring resistance to cucumber mosaic virus requires salicylic acid, ethylene and a novel signal transduction mechanism. Plant J. 32, 655–667.

Takahashi, H., Kanayama, Y., Zheng, M.S., Kusano, T., Hase, S., Ikegami, M., Shah, J., 2004. Antagonistic interactions between the SA and JA signaling pathways in Arabidopsis modulate expression of defense genes and gene-for-gene resistance to cucumber mosaic virus. Plant Cell Physiol. 45, 803–809.

Taraporewala, Z.F., Culver, J.N., 1996. Identification of an elicitor active site within the three-dimensional structure of the tobacco mosaic tobamovirus coat protein. Plant Cell 8, 169–178.

Van der Biezen, E.A., Jones, J.D., 1998. Plant disease-resistance proteins and the gene-for-gene concept. Trends Biochem. Sci. 23, 454–456.

Weber, H., Schultze, S., Pfitzner, A.J., 1993. Two amino acid substitutions in the tomato mosaic virus 30-kilodalton movement protein confer the ability to overcome the Tm-2(2) resistance gene in the tomato. J. Virol. 67, 6432–6438.

Weiner, S.J., Kollman, P.A., Case, D.A., U. Singh, C., Ghio, C., Alagona, G., Profeta, S., Weiner, P., 1984. A new force field for molecular mechanical simulation of nucleic acids and proteins. J. Am. Chem. Soc. 106, 765–784.

White, J.L., Kaper, J.M., 1989. A simple method for detection of viral satellite RNAs in small tissue samples. J. Virol. Methods 23, 83–94.

Zheng, M.S., Takahashi, H., Miyazaki, A., Hasamoto, H., Shah, J., Yamaguchi, I., Kusano, T., 2004. Up-regulation of *Arabidopsis thaliana* NHL10 in the hypersensitive response to Cucumber mosaic virus infection and in senescing leaves is controlled by signalling pathways that differ in salicylate involvement. Planta 218, 740–750.